

Beam Asymmetry in $\gamma n \rightarrow \pi^- p$ from CLAS-g13 data

D. Sokhan, D. Watts

University of Edinburgh, Edinburgh EH9 3JZ, UK

N. Benmouna, F.J. Klein (contact person), J.P. Santoro, D.I. Sober

The Catholic University of America, Washington, DC 20064

W.J. Briscoe, I.I. Strakovsky, R.L. Workman

The George Washington University, Washington, DC 20052

M. Dugger, E. Pasyuk, B.G. Ritchie

Arizona State University, Tempe, AZ 85287

Abstract

Our knowledge on baryon spectroscopy is largely based on the multipole analyses of the πN channel. Moreover, our knowledge for photocouplings of these resonances is as well largely based on pion (photo-) production data. However, almost all data on πN and γN were taken on proton targets, thus neutron couplings are largely unknown – in particular for higher mass resonances. Due to the isoscalar and isovector nature of the electromagnetic field both proton and neutron data are required to determine the coupling parameters of N^* resonances.

We propose to analyze CLAS-g13 data [1] with regard to the reaction $\gamma n \rightarrow \pi^- p$. CLAS-g13 provides the opportunity for analyzing this reaction without requesting additional beam time. Data being taken for $K^0 \Lambda$ provide enough statistics for the pion channel. Of special interest is the data set with linearly polarized photons, which allows for extracting the beam asymmetry Σ_x . The projected yield for CLAS-g13b data is sufficiently large to extract Σ_x in the photon energy range from 1.1 to 2.3 GeV in bins of $\Delta E_\gamma=50$ MeV and 9 bins in $\cos \theta_{cm}$ from -0.8 to almost +1.0. Cross section data will be extracted as well in order to study systematics. However, the large data set of CLAS-g10 has already been analyzed with regard to single pion production [2]; these results are expected to dominate the cross section data on $\gamma n \rightarrow \pi^- p$.

1 Motivation

One of the most challenging topics in subnuclear physics is the study of the structure of the nucleon and its modes of excitation. In a naive description, proton and neutron only differ by the exchange of one u and d quark, thus resulting in isospin invariance for strong interaction. However, in the deep inelastic regime the ratio of u and d quark structure functions is not unity. It is not expected that this is the case in the non-perturbative regime of QCD. In this regime various attempts are made to provide a phenomenological description of experimental data. In general, predictions of such models are questionable in kinematical regimes where no (or scarce) experimental data is available. Experimental data for each isospin partner is crucial to provide a deeper understanding of the governing physics.

Due to its comparatively large cross section and easy experimental access pion production has been studied for a long time, and this has been the primary source of established N^* and Δ^* parameters, like mass, spin, width, pole position, and – to some extent – photo-coupling. However, our knowledge of the baryon spectrum is still very limited. This is largely due to the complexity of the nucleon resonance spectrum, with many broad, overlapping resonances coupling to πN . In the low energy regime the analysis of pion reactions on proton targets has been sufficient since multipole phases are related by Watson’s theorem. However, with the onset of inelasticity, i.e. above the 2-pion threshold, the multipole analyses becomes model-dependent. Photoproduction data are fitted to models that incorporate resonant and non-resonant (background) production and are constrained by PWA results of πN data.

While most phenomenological approaches attempt to describe the experimental data using effective Lagrangians on the tree level and determine resonance parameters by fitting to experimental data, the SAID approach first obtains multipole amplitudes in a least model dependent way (“single energy solution”), with the number of included multipoles depending on the experimental data. Then the extracted multipoles are refitted to functional forms having both resonance and background contributions in an energy dependent (global) fit to the data. Note that this procedure requires not only cross section data but many polarization

data in order to constrain the solution. For the beam asymmetry in $\gamma n \rightarrow \pi^- p$, in particular, only few data points exist from the ‘‘Moby Dick’’ spectrometer at a center-of-mass angle of 90° [5] and from two-arm spectrometer experiments at Yerevan [6, 7]. As shown in Fig. 1 the existing data points are well described by the recent SAID solution [3] though the functional form is not well constrained by the few data points. The MAID solution [4], however, differs significantly from the SAID solution as well as the existing data.

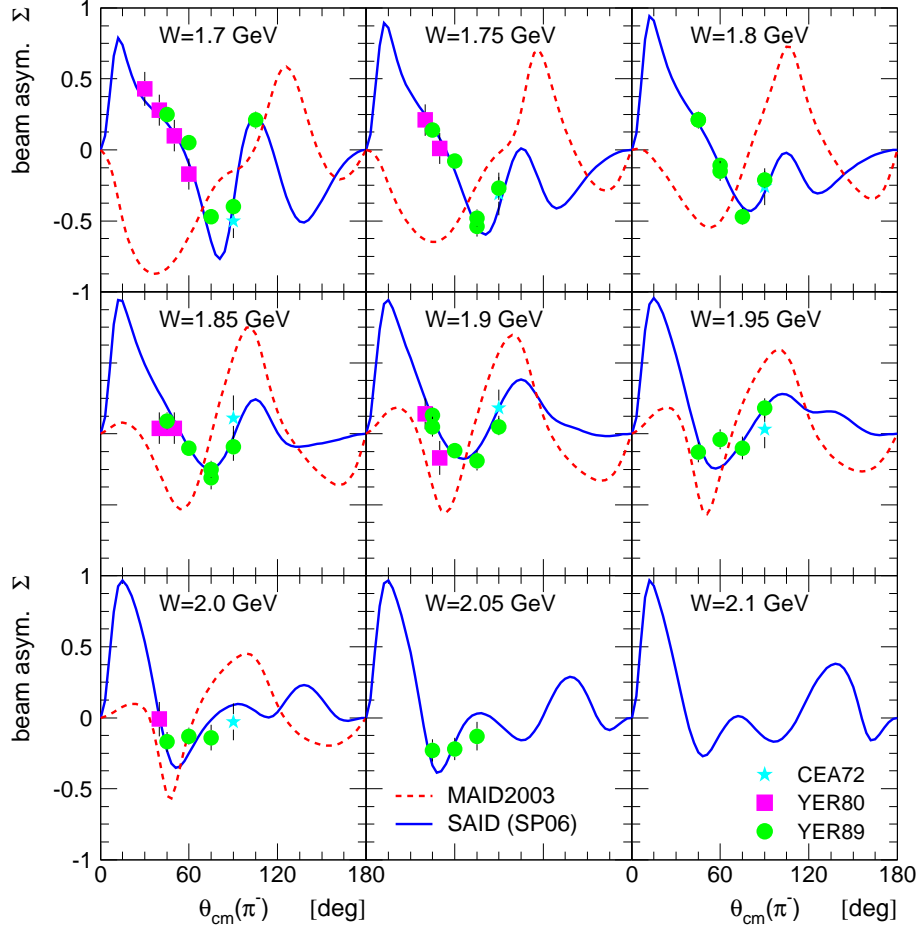


Figure 1: Existing data for beam asymmetry in $\gamma n \rightarrow \pi^- p$ and recent solutions from SAID [3] and MAID [4]. The PWA solutions are plotted for the corresponding c.m. energy W , whereas all experimental data point in the energy range $W \pm 25$ MeV are plotted.

Over the last 10+ years the progress in experimental techniques and high precision data allowed to determine the properties of $\Delta(1232)$ very well. However, the analyses of higher excitation states requires data of all four $\gamma N \rightarrow \pi N$ channels and the inclusion of other reactions. In order to completely determine the amplitudes for photoproduced pions, data for both proton and neutron targets are required. This requirement arises from the isoscalar and isovector nature of the photon field:

$$A_{\gamma p \rightarrow \pi^0 p} = - \left[\frac{1}{3} A_{\pi N}^{(0)} - \frac{1}{3} A_{\pi N}^{(1)} \right]^{(I=\frac{1}{2})} + \frac{2}{3} A_{\pi N}^{(I=\frac{3}{2})} \quad (1)$$

$$A_{\gamma p \rightarrow \pi^+ n} = \frac{1}{\sqrt{2}} \left[\frac{1}{3} A_{\pi N}^{(0)} - \frac{1}{3} A_{\pi N}^{(1)} \right]^{(I=\frac{1}{2})} + \frac{\sqrt{2}}{3} A_{\pi N}^{(I=\frac{3}{2})} \quad (2)$$

$$A_{\gamma n \rightarrow \pi^0 n} = \left[\frac{1}{3} A_{\pi N}^{(0)} + \frac{1}{3} A_{\pi N}^{(1)} \right]^{(I=\frac{1}{2})} + \frac{2}{3} A_{\pi N}^{(I=\frac{3}{2})} \quad (3)$$

$$A_{\gamma n \rightarrow \pi^- p} = -\frac{1}{\sqrt{2}} \left[\frac{1}{3} A_{\pi N}^{(0)} + \frac{1}{3} A_{\pi N}^{(1)} \right]^{(I=\frac{1}{2})} + \frac{\sqrt{2}}{3} A_{\pi N}^{(I=\frac{3}{2})} \quad (4)$$

The components $A^{(0)}$ and $A^{(1)}$ result from coupling of the $I=\frac{1}{2}$ nucleon to the isoscalar and isovector component of the photon field to yield a total isospin of $\frac{1}{2}$. Note that measurements of $\gamma p \rightarrow \pi^0 p$ and $\gamma p \rightarrow \pi^+ n$ are sufficient to isolate the $I=\frac{3}{2}$ amplitudes, but measurements on the proton channels are insufficient to disentangle $A^{(0)}$ and $A^{(1)}$. This can only be accomplished by additional measurements on a neutron channel.

2 Simulation

In order to determine the acceptance for the reaction $\gamma n \rightarrow \pi^- p$ and to investigate the separation of this channel from background reactions as well as the separation from rescattering contributions, we simulated the elementary process using the 2006 SAID solution [3] and smeared the result to account for the momentum distribution $\rho(\vec{p}_s)$ of the spectator and the moving target nucleon in order to describe quasi-free production:

$$\frac{d^5\sigma}{dp_s d\Omega_{p_s} d\Omega_\pi} = \left(1 + \frac{p_s}{E_s} \cos \theta_{p_s}\right) \rho(\vec{p}_s) \frac{d^2\sigma}{d\Omega_\pi}(\gamma n \rightarrow \pi^- p) . \quad (5)$$

The simulation package `genbos`, which includes the Paris potential for $\rho(\vec{p}_s)$, was used to generate quasi-free events, which were then fed into the `geant` Monte Carlo simulation program for CLAS (`gsim`) and the reconstruction program `user_ana`. Two sets of 400,000 events for $E_\gamma = 1250 \pm 50$ MeV were uniformly produced over the length of the 40 cm deuterium target, centered at $z = -20$ cm, with the torus field set to -1500 A – as being used in CLAS-g13. The angular distribution of the thrown events followed the differential cross section and beam asymmetry from the SAID solution as follows [8]:

$$N(d\Omega) = N_0(\cos \theta_{cm}) (1 - P_{lin} \Sigma \cos 2\varphi) . \quad (6)$$

N_0 denotes rate based on the unpolarized cross section, N the rate modulated by the photon polarization. For the first set the photon beam was assumed to be 90% polarized in the horizontal plane, i.e. $\varphi = \phi_{lab}(\pi^-)$, $P_{lin} = 0.9$; for the second set to 90% polarized in the vertical plane, i.e. $\varphi = \phi_{lab}(\pi^-) - \frac{\pi}{2}$. Background for 2-pion production ($\gamma p \rightarrow \pi^+ \pi^- p$ and $\gamma n \rightarrow \pi^0 \pi^- p$) were produced as quasi-free processes (unpolarized distributions only) with 400,000 and 100,000 events, respectively.

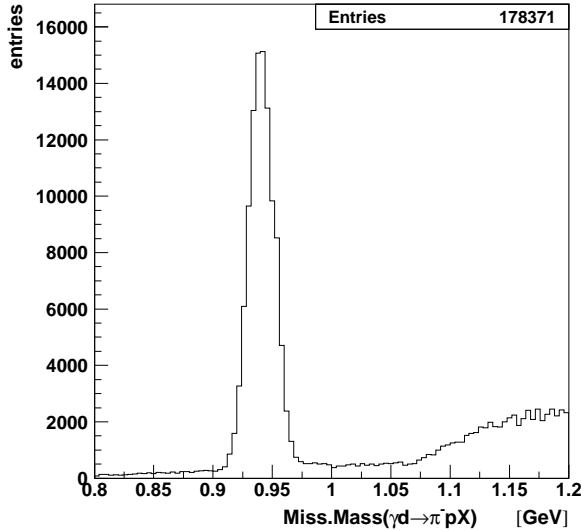


Figure 2: Missing mass distribution for $\gamma d \rightarrow \pi^- p X$ (simulated data). The reaction $\gamma n \rightarrow \pi^- p$ is identified by means of the cut $MM(\gamma d \rightarrow \pi^- p X) < 1.0$ GeV.

The reaction $\gamma n \rightarrow \pi^- p$ is identified via a missing mass cut on the spectator after identifica-

tion of a single reconstructed π^- and proton in the event, as shown in Fig. 2. The missing momentum distribution of the resulting event sample and the distribution of the relative azimuthal directions of proton and π^- are shown in Fig. 3. A cut on the missing momentum $p_{miss}=p_s < 200$ MeV and the back-to-back direction of proton and π^- are used to determine the quasi-free process.

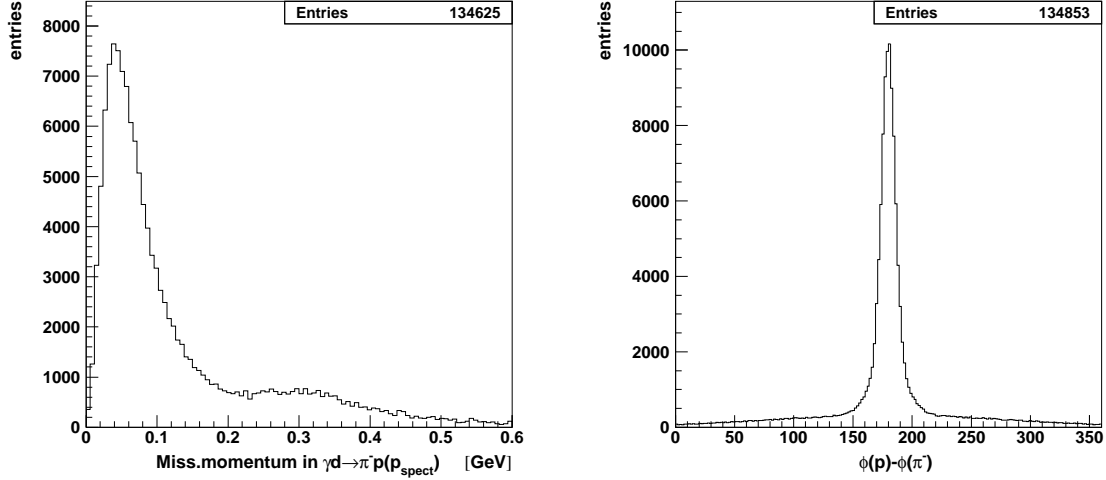


Figure 3: Missing momentum for $\gamma d \rightarrow \pi^- p X$ and coplanarity of π^- and proton (simulated data) after the missing mass cut was applied. A cut on the spectator momentum $p_{miss} < 200$ MeV and the coplanarity ($160^\circ < \Delta\phi < 200^\circ$) defines the quasi-free process.

Fiducial cuts were used to eliminate reconstructed tracks in the region of the torus coils. These cuts turned out to be important since our earlier studies showed that the acceptance is not well understood in these regions caused by inaccurate track reconstruction near the coil positions. Our previously chosen binning of $\Delta\phi=20^\circ$ was so coarse that we obtained decent statistics even near the coil regions since we did not apply fiducial cuts. We note that such fiducial cuts are being used for real data as well. Figures 4 and 5 show the azimuthal distribution of reconstructed $\pi^- p(p_s)$ events for 9 bins in $\cos\theta_{cm}$ for both sets of simulated events. A fit to the reconstructed yields using the function $f(\phi) = P_1\{1 - P_2 \cos[2(\phi - P_3)]\}$ provides the extracted beam asymmetry as function of $\cos\theta_{cm}$ with $P_2=P_{lin}\Sigma$.

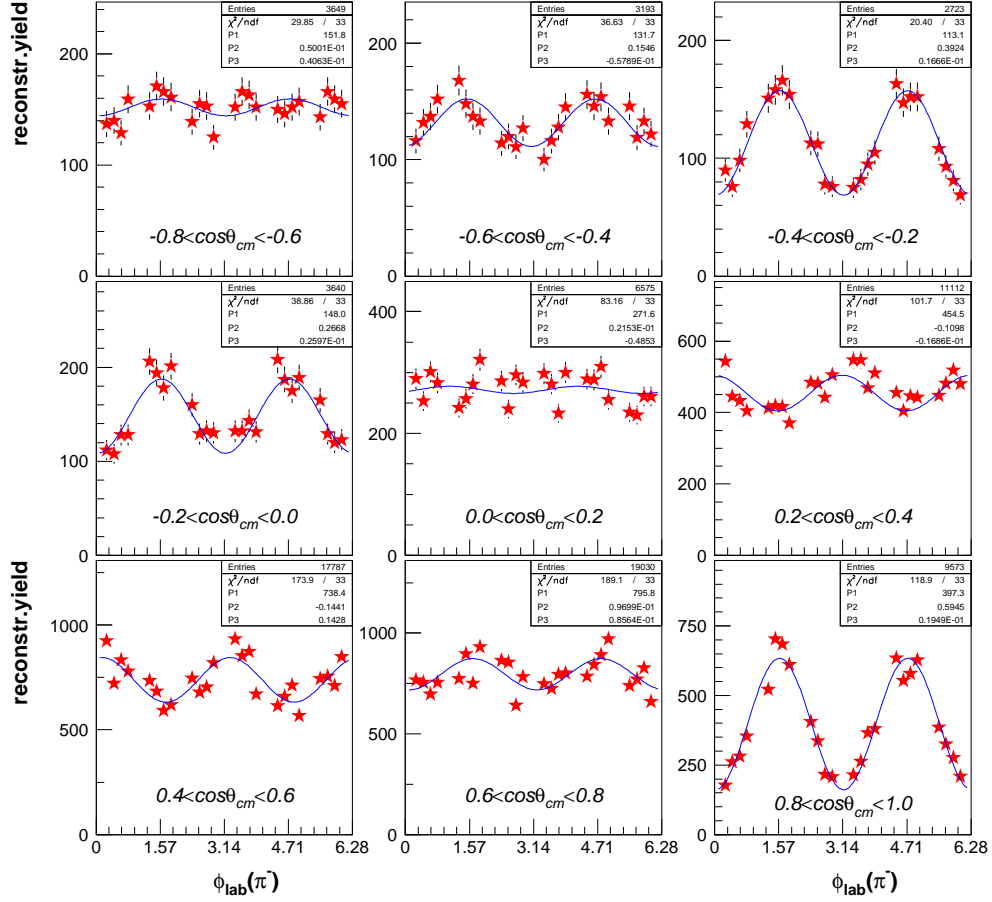


Figure 4: Reconstructed yields from simulated events with horizontal photon polarization. The azimuthal distributions for 9 bins in $\cos\theta_{\text{cm}}$ show a ϕ modulation, which is fitted to the function $f(\phi) = P_1\{1 - P_2 \cos(2(\phi - P_3))\}$.

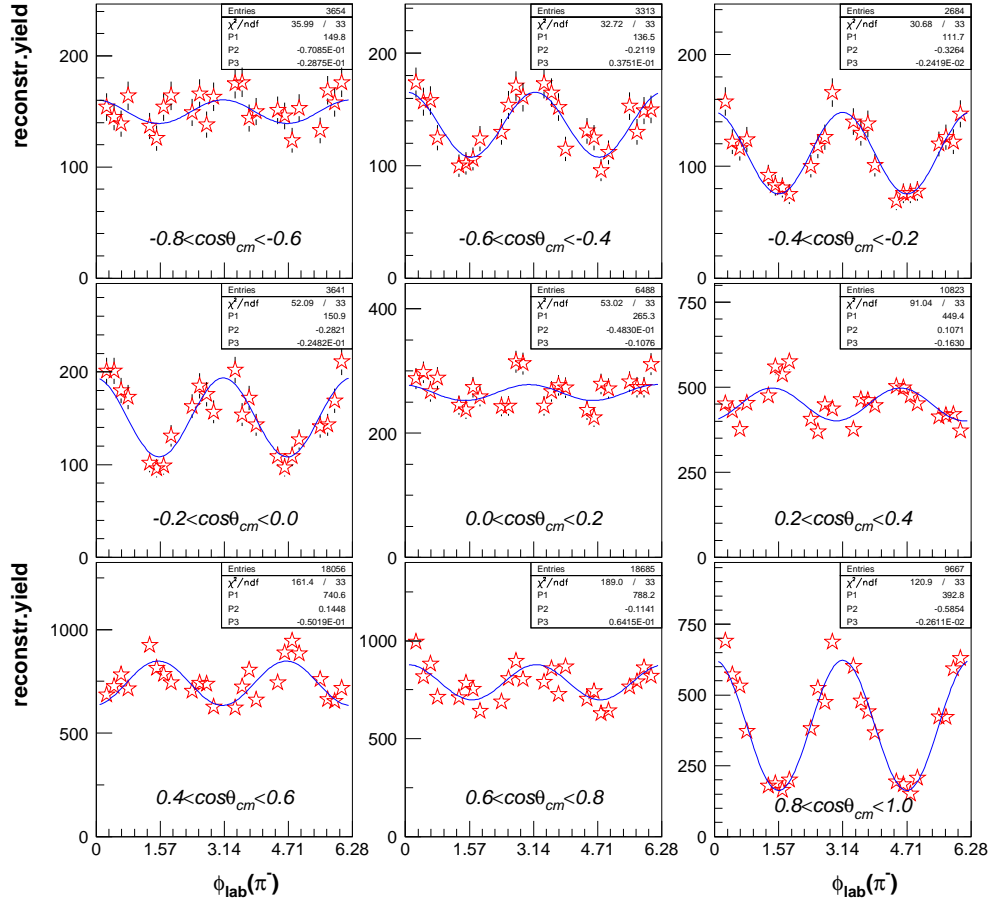


Figure 5: Reconstructed yields from simulated events with vertical photon polarization. The azimuthal distributions for 9 bins in $\cos\theta_{cm}$ show a ϕ modulation, which is fitted to the function $f(\phi) = P_1\{1 - P_2 \cos(2(\phi - P_3))\}$.

The choice of small bins in ϕ ($\Delta\phi=10^\circ$) allowed for a comparatively reliable fit to extract the beam asymmetry without relying on both data sets as shown in Fig. 6. The beam asymmetry from each data set reproduces the generated function within the errors. The independent analysis of the data sets with horizontal (parallel) and vertical (perpendicular) photon polarization, however, provides a means to study the systematics. We note that the simulated statistics would have been sufficient to extract Σ for smaller intervals in E_γ and $\cos\theta_{cm}$, which would require to combine the data sets.

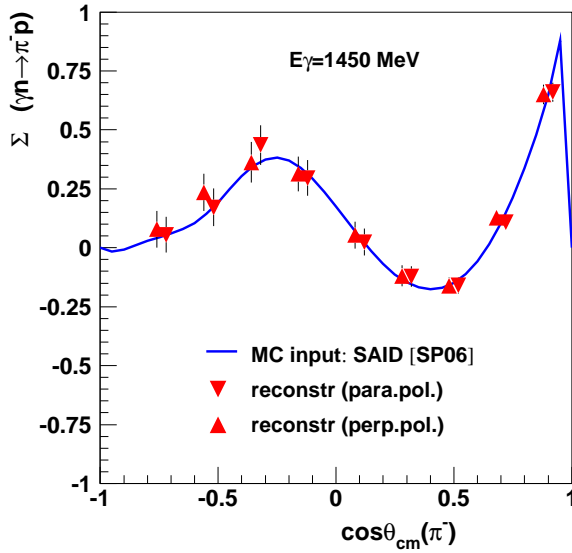
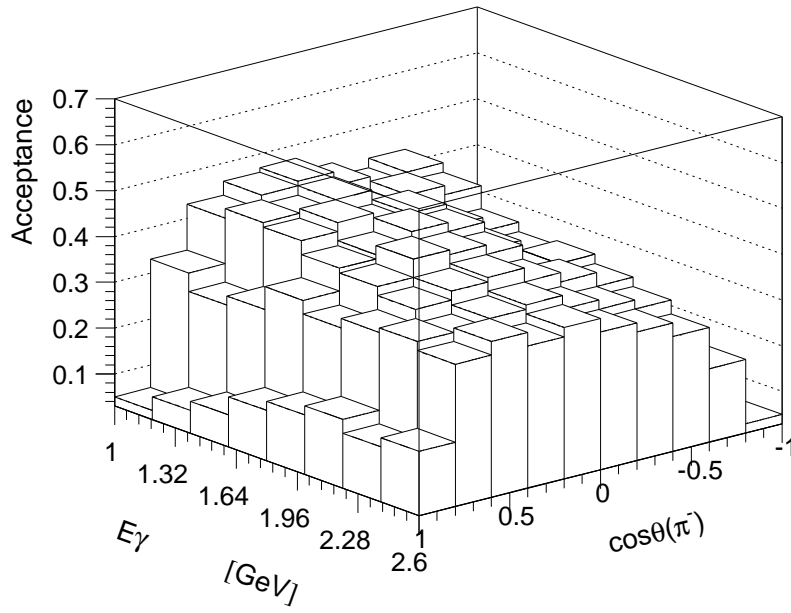


Figure 6: Extracted beam asymmetry from the fit to the azimuthal distributions shown in Fig. 4 for horizontal photon polarization and in Fig. 5 for vertical photon polarization. The curve represents the generated distribution, which followed the SAID solution of 2006 [3].

Additional data for $\gamma n \rightarrow \pi^- p$ in the photon energy from 1.0 to 2.6 GeV were generated to obtain an acceptance table, as shown in Fig. 7. The acceptance simulation will be repeated with higher statistics using the calibration results of g13 data.

Figure 7: Acceptance for quasi-free $\gamma n \rightarrow \pi^- p$ over a larger energy range.

3 Summary of the analysis of $\gamma n \rightarrow \pi^- p$ from g10 data

The analysis of $\gamma n \rightarrow \pi^- p$ from g10 data, taken in spring of 2004, is going to be under CLAS internal review in 2007. Out of 3.2 billion events taken on a 25 cm long deuterium target with high torus field ($I_{torus}=3375$ A) and 620 Million events with lower torus field ($I_{torus}=2250$ A) final data sets were obtained through a series of cuts: Besides the standard selection of runs with stable beam and detector conditions, the cuts included: (i) vertex cut, (ii) fiducial cuts, (iii) good timing of beam photon, pion, and proton ($\Delta t < 1$ ns), (iv) missing mass cut to identify the spectator proton (initially $|M_X - m_p| < 0.1$ GeV, final cut $|M_X - m_p| < 3\sigma$ of the peak width), and (v) missing momentum cut ($P_X < 0.2$ GeV). After applying these cuts the final data set comprised of 26 Million events for the high field data and 5 Million for the lower field data. We note that the acceptance for $\gamma n \rightarrow \pi^- p$ in g10, as plotted in Fig. 8 for one energy bin, is about 20% lower than ours and misses the very forward direction, due to unfavorable torus field settings and malfunctioning detector components.

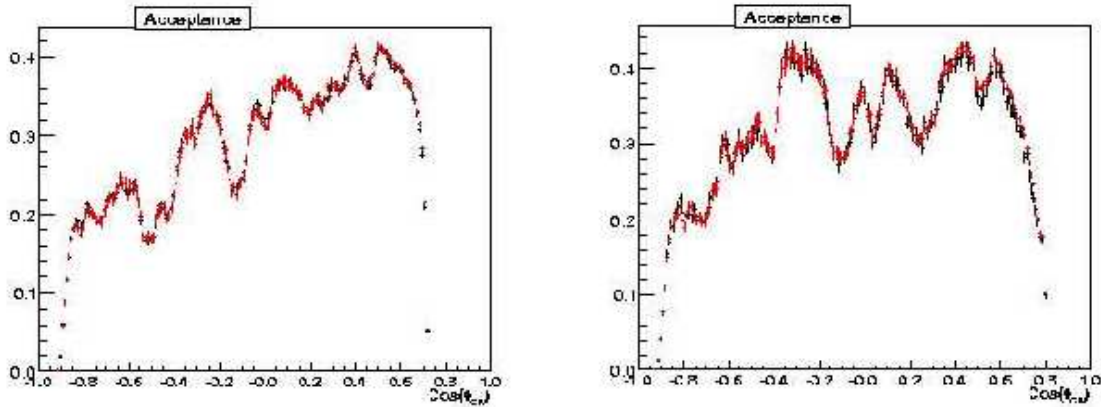


Figure 8: g10 data: acceptance for quasi-free $\gamma n \rightarrow \pi^- p$ at $E_\gamma=1.25$ GeV, *left* for the high field data ($I_{torus}=3375$ A), *right* for the lower field data ($I_{torus}=2250$ A). The acceptance for MC data from different generators is shown in different colors (from [2]).

4 Exploratory analysis and expected yields from g13 data

In the run period with circularly polarized photons in the fall of 2006, almost 10.5 billion events were collected during the first part of the run with $E_0=1.99$ GeV and around 8.5 billion events during the second part with $E_0=2.65$ GeV. Data taking with plane-polarized photons from a $50\mu\text{m}$ thin diamond oriented in a goniometer started in March 2007. The degree of polarization depends on the fractional photon energy (E_γ/E_0) and tight collimation. We expect photon polarizations of 80-90%.

Data from a single run in March'07, for which the coherent edge was set to 1.3 GeV, yielded an azimuthal distribution for horizontal polarization direction as shown in Fig. 9 after normalizing the polarized yield with amorphous data.

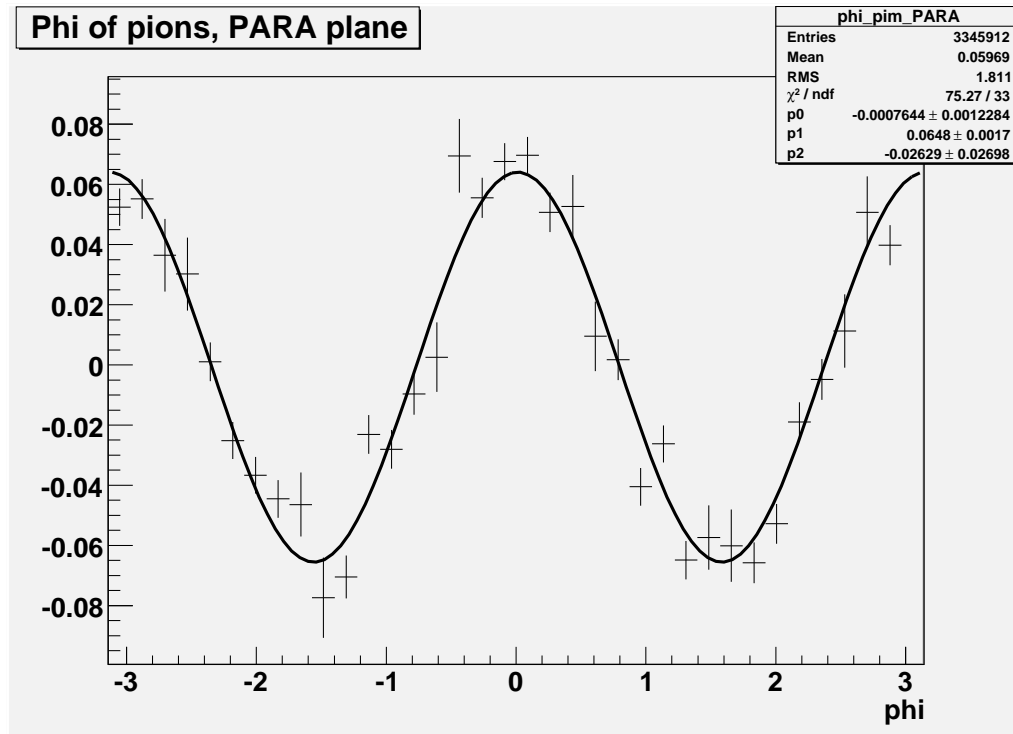


Figure 9: g13 data (run 54125): Phi distribution of normalized yield for horizontal photon polarization in the energy range of 1.1 to 1.3 GeV.

The expected rates in Table 1 is based on a photon flux of 12 MHz on target as achieved during g8b and the beam time allocated for g13. For the tabulated degree of photon beam polarization (P_{lin}) we assumed an electron energy of $E_0 \simeq 4.5$ GeV, however due to the high yields lower beam energies and correspondingly lower photon polarization would not diminish the outcome of this analysis. Based on the fitted differential cross section, a target length of 40 cm, and our acceptance study, we estimate the $\gamma n \rightarrow \pi^- p$ yield from g13 data with linearly polarized photons as shown in Fig. 10.

We expect that the uncertainty of our results will be dominated by systematic uncertainties of about 5-6%, with major contributions from background subtraction ($\approx 2\%$) and photon beam polarization (4-5%).

Table 1: Approximate yield of reconstructed $\gamma n \rightarrow \pi^- p$ events during the g13 run with linearly polarized beam ($E_0 \simeq 4.5$ GeV is assumed for P_{lin}).

E_γ (GeV)	P_{lin}	beam time	projected yield	bins $\Delta E \times \Delta \cos \theta$
1.1 – 1.3	92%	5 days	950k	4×18
1.3 – 1.5	90%	4 days	600k	4×18
1.5 – 1.7	88%	5 days	700k	4×18
1.7 – 1.9	85%	6 days	800k	4×18
1.9 – 2.1	82%	6 days	700k	4×18
2.1 – 2.3	79%	7 days	650k	4×18

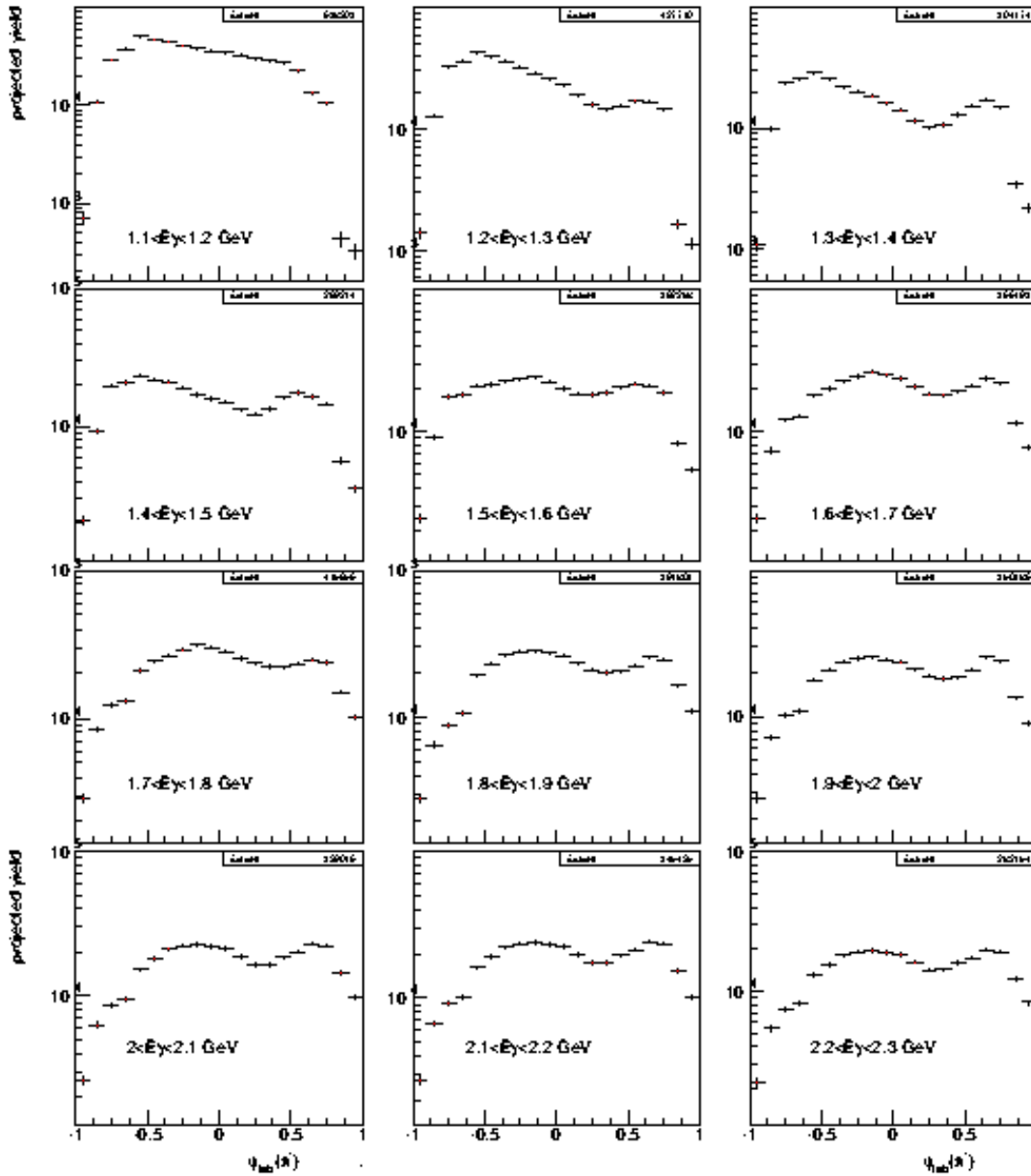


Figure 10: Yield estimates for $\gamma n \rightarrow \pi^- p$ during the g13 run period with linearly polarized photons. These estimates are based on the requested beam time and our simulation studies. More accurate estimates from g13b data taking will be available in late summer 2007.

References

- [1] P. Nadel-Turonski, B.L. Berman, Y. Ilieva, A. Tkabladze, D.G. Ireland, “Kaon Production on the Deuteron Using Polarized Photons”, Jefferson Lab Experiment E06-103 (2006).
- [2] W. Chen, D. Dutta, H. Gao, T. Mibe, *et al.*, “Measurement of differential cross sections for $\gamma n \rightarrow \pi^- p$ reaction”, CLAS g10 analysis (2004-2007).
- [3] R.A. Arndt, W.J. Briscoe, I.I. Strakovski, and R.L. Workman, Phys. Rev. C **66**, 055213 (2002); see SP06 at <http://gwdac.phys.gwu.edu>.
- [4] D. Drechsel, O. Hanstein, S.S. Kamalov, and L. Tiator, Nucl. Phys. **A645**, 145 (1999); see MAID03 at <http://www.kph.uni-mainz.de/MAID>.
- [5] J. Alspector, *et. al.*, Phys. Rev. Lett. **28**, 1403 (1972).
- [6] L. Abrahamian, *et. al.*, Sov. J. Nucl. Phys. **32**, 69 (1980).
- [7] F. Adamyan, *et. al.*, J. Phys. **G 15**, 1797 (1989).
- [8] G. Knöchlein, D. Drechsel, and L. Tiator, Z. Phys. **A352**, 327 (1995).